Generation of Size-Controlled, Submicrometer Protein Crystals

Joshua C. Falkner,[†] Ali M. Al-Somali,[†] Jennifer A. Jamison,[†] Junyan Zhang,[†] Stephanie L. Adrianse,[†] Rhoniese L. Simpson,[†] Michelle K. Calabretta,[‡] Wilson Radding,[§] George N. Phillips, Jr.,[§] and Vicki L. Colvin*[,†]

Departments of Chemistry and Biochemistry, MS-140 Rice University, 6100 Main St, Houston, Texas 77005 and Department of Biochemistry, University of Wisconsin−Madison, Room 6607, 433 Babcock Drive, Madison, Wisconsin 53706-1544

Received November 29, 2004

Cross-linked protein crystals represent a new class of micro- and mesoporous materials with properties potentially useful in technologies as diverse as chiral separations and drug delivery. These applications require the generation of protein crystals in formats and sizes quite distinct from the traditional submillimeter single crystals favored by structural biologists. Here we report a high-yield method for forming monodisperse protein crystals with tunable dimensions ranging from 250 nm up to tens of micrometers. X-ray powder diffraction of these crystallites confirms that the hen egg white lysozyme crystals are identical in structure to that of the bulk tetragonal lysozyme ($a = 79.05$ Å; $c = 37.96$ Å).

I. Introduction

Interest in biomolecular crystals over the past century has been driven by their immense value to structural biology which uses large (0.1−0.5 mm) high-quality protein crystals to resolve biomolecular structures at the 1−3 Å level.[1] Protein crystals have also recently been identified as valuable materials beyond their applications in biological research. They are porous solids with ordered voids which can be considered analogous to inorganic zeolites. Recently protein crystal systems have been used for various purposes including catalysis and drug delivery.[2,3] With the interest in these systems expanding rapidly, various methods which permit optimization of protein crystal format (e.g., size, shape, support) are needed. In particular, much like inorganic porous solids, the physical size of a biomolecular crystal should be central to defining its performance in many applications.[4,5] Smaller protein crystals not only would have improved mass transport to interior pores for more efficient catalysis, but also, as with drug delivery, may provide alternative routes of administration and release properties. In this work we demonstrate a method to produce small, size-tunable, high-quality protein crystals with narrow size distributions using hen egg white lysozyme as a model system. To achieve this result we crystallize materials in a different part of the protein solubility phase diagram than conventional routes. Through precise control of initial protein concentration and parameters that control protein solubility such as pH, temperature, and precipitant concentration, we can dictate size from a few hundred nanometers up to tens of micrometers.

The prime motivating factor of this study, to control protein crystallization, stems from the enormous possibilities these materials provide for materials chemistry. Central to their use is the fact that these biomolecular crystals contain well-ordered interpenetrating micro- and, in some cases, mesoporous solvent channels. These channels provide a chemically heterogeneous and chiral environment which comprises 30−65% of the total crystal volume.[6] In lysozyme, the model system for this work, the pore diameter ranges from 1 to 2.5 nm in a series of linked major and minor pores. Figure 1 shows the major porous structure of a hen egg white lysozyme (HEWL) crystal generated from standard crystallographic information for the tetragonal crystal structure, where the pores are aligned along the *c*-axis of the unit cell within the crystal.

Most applications for protein crystals require a secondary cross-linking step that is necessary due to the poor mechanical properties and stability of un-cross-linked crystals. Crystals are treated with compounds such as glutaraldehyde to form covalent bonds between key amino acid functionalities within the structure.[3,7,8] In the case of HEWL, this treatment only slightly degrades the crystal quality and provides samples that can be easily handled and even dehydrated. Cross-linked protein crystals (CLPC)s have also been shown to be resilient under high shear conditions encountered in both fluid transfer and agitation.[2,3,9−14] One

* To whom correspondence should be addressed.
[†] Department of Chemistry, Rice University.
[‡] Department of Biochemistry, Rice University.
[§] Department of Biochemistry, University of Wisconsin−Madison.

(1) Lin, T. W.; Johnson, J. E. Structures of picorna-like plant viruses: Implications and applications. In *Advances in Virus Research;* Maramorosch, K., Murphy, F. A., Shatkin, A. J., Eds.; Elsevier Academic Press Inc.: San Diego, CA, 2003; Vol. 62, pp 167−239.
(2) Margolin, A. L.; Navia, M. A. *Angew. Chem., Int. Ed.* **2001**, *40* (12), 2205−2222.
(3) Margolin, A. L. *Trends Biotechnol.* **1996**, *14* (7), 223−230.
(4) Reding, G.; Maurer, T.; Kraushaar-Czarnetzki, B. *Microporous Mesoporous Mater.* **2003**, *57* (1), 83−92.
(5) Aerts, A.; van Isacker, A.; Huybrechts, W.; Kremer, S. P. B.; Kirschhock, C. E. A.; Collignon, F.; Houthoofd, K.; Denayer, J. F. M.; Baron, G. V.; Marin, G. B.; Jacobs, P. A.; Martens, J. A. *Appl. Catal. A: Gen.* **2004**, *257* (1), 7−17.
(6) Matthews, B. W. *J. Mol. Biol.* **1968**, *33*, 491−497.
(7) Walt, D. R.; Agayn, V. I. *Trac-Trends Anal. Chem.* **1994**, *13* (10), 425−430.
(8) Tashima, T.; Imai, M.; Kuroda, Y.; Yagi, S.; Nakagawa, T. *J. Org. Chem.* **1991**, *56* (2), 694−697.

10.1021/cm047924w CCC: $30.25
Published on Web 04/22/2005

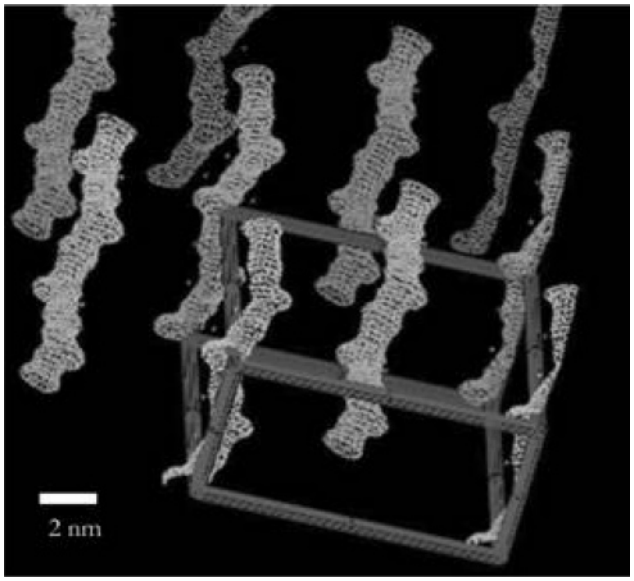

Figure 1. Major solvent channels of tetragonal lysozyme that run throughout the crystal. The image was generated from XRD data of HEWL taken from the Brookhaven Protein Data Bank.[23] The box in this figure encompasses one unit cell.

company even provides these materials commercially as cross-linked enzyme crystals (CLEC)s where the cross-linking of the proteins provides an avenue for improved drug delivery of protein therapeutics.[15]

The reported applications for protein crystals have expanded substantially in the past 5 years. In most applications crystallite grain size—both absolute size as well as tunability—is central to material performance. Vilenchik et al. noted that for enzyme catalysis smaller crystals would be more efficient because of enhanced mass transfer to active surfaces, and their work showed improved performance in 5 μm as compared to larger crystallites.[13] The impact of these materials in the area of catalysis is far reaching.[3] For example, enzyme crystals have been used to produce high-fructose corn syrup,[16] synthesize peptides,[12] and form C−C bonds.[17] Cross-linked protein crystals have also been developed as stationary phases for a number of different modes of chromatographic separation. A reduction in grain size of the stationary phase would lead to less column dead volume and a greater enhancement in the resolution of a chromatogram.[18] Using thermolysin-CLEC's researchers were able to resolve compounds based on size-exclusion separations of different molecular weight PEG molecules, adsorption separations of (*S*)-ibuprofen and (*R*)-phenyllactic acid, and chiral separations of (*S*)- and (*R*)-phenylglycine.[13] More recently protein crystals have been utilized in drug delivery for protein therapeutics.[2,19] In this arena, the development of small-sized protein crystals is particularly attractive as it may permit delivery routes that are not practical for sub-millimeter-sized materials.

This paper reports for the first time a method to make size-controlled micrometer and submicrometer protein crystals with high yield and good quality. Rather than relying on quenching to limit crystal growth, we optimized conditions to favor a large number of very small nuclei. This requires that we operate in a different part of the crystal growth phase diagram than conventional crystallographers, namely, at conditions which favor extremely low protein solubility. Crystallization under these conditions has never before been examined, and we show that for HEWL the nucleation in this regime is well separated from growth, and extremely monodisperse (σ < 10%) particles are the result.

II. Experimental Section

Materials. High-purity freeze-dried hen egg white lysozyme (Calzyme Laboratories Inc.; 50 000 U/mg) was used for this work. Because it was determined by SDS−Page gel electrophoresis that this reagent contained no other protein impurities, no further purification was necessary. Glacial acetic acid, sodium hydroxide, and sodium chloride were purchased from Fisher Scientific. Poly(ethylene glycol) (PEG), MW = 6000, was purchased from Fluka Chemika. Gutaraldehyde, 50 vol %, was purchased from Sigma-Aldrich. All solutions were prepared using ultrapure water (18.2 MΩ resistivity).

Crystallization Buffers. All crystallization buffers contained 0.5 M acetate/acetic acid prepared from glacial acetic acid. After addition of all other reagents, each buffer was adjusted to the desired pH by titration with 10 M NaOH. For protein buffers, hen egg white lysozyme concentration was determined by absorbance at 280 nm using an extinction coefficient of $\alpha^{280\text{nm}} = 2.64$ mL mg^{-1} cm^{-1} with a Varian, Cary 5000 ultra-violet visible spectrometer.[20] Before use, buffers that contained lysozyme were centrifuged for 10 min at 6400*g* in order to remove any undissolved protein. Precipitant buffers of varying concentrations of both sodium chloride and PEG 6000 were prepared based on weight per volume (w/v) calculations.

Crystal Growth. A modified batch method was used for all crystallizations. Because of the high concentrations of salt required, a 3:1 volume ratio of precipitant buffer to protein buffer was used instead of the standard 1:1 ratio. Screening batches of 1 mL were set up in 24-well Hampton Research VDX plates. Scale-up batches were also produced in 125 mL Wheaton glass bottles. To ensure faster and homogeneous mixing, these scale-up batches were vigorously stirred using a magnetic stir bar during the transfer of buffers. All batches were prepared by rapidly combining the precipitant buffer to the protein buffer. Then the batches were sealed and allowed to grow for a 24-h period in a temperature-controlled environment (±1 °C). Parameters adjusted for crystallization conditions included protein concentration (1−8 mg/mL), pH (3.0−4.5), temperature (1−24 °C), NaCl concentration (5−18%), PEG 6000 concentration (0−6%), and batch volume (1−50 mL).

(9) Govardhan, C. P.; Margolin, A. L. *Chem. Ind.* **1995**, (17), 689−693.
(10) Khalaf, N.; Govardhan, C. P.; Lalonde, J. L.; Persichetti, R. A.; Wang, Y. F.; Margolin, A. L. *J. Am. Chem. Soc.* **1996**, *118* (23), 5494−5495.
(11) Lalonde, J. J.; Govardhan, C.; Khalaf, N.; Martinez, A. G.; Visuri, K.; Margolin, A. L. *J. Am. Chem. Soc.* **1995**, *117* (26), 6845−6852.
(12) Persichetti, R. A.; Stclair, N. L.; Griffith, J. P.; Navia, M. A.; Margolin, A. L. *J. Am. Chem. Soc.* **1995**, *117* (10), 2732−2737.
(13) Vilenchik, L. Z.; Griffith, J. P.; St Clair, N.; Navia, M. A.; Margolin, A. L. *J. Am. Chem. Soc.* **1998**, *120* (18), 4290−4294.
(14) Wang, Y. F.; Yakovlevsky, K.; Margolin, A. L. *Tetrahedron Lett.* **1996**, *37* (30), 5317−5320.
(15) http://www.altus.com/.
(16) Visuri, K. European Patent 0341503, 1989.
(17) Sobolov, S. B.; Bartoszkomalik, A.; Oeschger, T. R.; Montelbano, M. M. *Tetrahedron Lett.* **1994**, *35* (42), 7751−7754.
(18) *Column Handbook for Size Exclusion Chromotography*; Academic Press: San Diego, CA, 1999.
(19) St Clair, N. L.; Shenoy, B.; Jacob, L. D.; Margolin, A. L. *Proc. Natl. Acad. Sci. U.S.A.* **1999**, *96* (17), 9469−9474.
(20) Sophianopoulos, A. J.; Rhodes, C. K.; Holcomb, D. N.; Van Holde, K. E. *J. Biol. Chem.* **1962**, *237*, 1107−1112.

Cross-Linking and Purification. After 24 h most solutions had visible evidence of protein crystallization. In some cases crystals in solution were easily seen by the naked eye, while in other cases a white haze signified crystallization. At this point each solution was centrifuged for 2 min at 2600*g*, and then the supernatant was removed. Each pellet was then resuspended with a cross-linking solution that was equal volume to the removed supernatant. This cross-linking solution consisted of 2.5% (w/v) glutaraldehyde in a buffer identical to the removed supernatant minus any protein. These samples were immediately removed from their temperature-controlled environment and equilibrated to room temperature (22−24 °C). After 48 h the crystals were purified by centrifugation. These cross-linked batches were centrifuged for 2 min at 2600*g*, and the yellowish pellet was resuspended in ultrapure water. This centrifugation/wash process was repeated three times.

Calculation of Crystallite Yields. The yields were approximated by analyzing the dissolved protein in the supernatant that was above the un-cross-linked protein crystal pellet after the first centrifugation. To ensure that no crystals were left in solution, the supernatant was removed and then recentrifuged (2 min, 2600*g*). An aliquot of the supernatant was taken and diluted to a known volume with ultrapure water to reduce the risk of further protein precipitation or crystallization. The absorbance was measured at 280 nm to determine the amount of protein that remained in the supernatant. A percent yield was calculated with the assumption that any protein not measured in the supernatant was crystallized.

Crystallite Analysis. Microscopy specimens were prepared by drying the aqueous solutions onto aluminum SEM specimen mount stubs from Electron Microscopy Sciences. Then a thin film of gold was sputtered onto the sample to reduce charging during electron microscopy. Images of the crystallites were obtained using a FEI XL-30 Environmental Scanning Electron Microscope operating at 30 kV. Image Pro Plus 5.0 from Media Cybernetics was used to facilitate the sizing of approximately 100−150 particles for each sample. Crystals were measured by width, which is defined as the distance between the {110} crystal surfaces, and length, which is defined as the distance between the apexes of the {101} crystal surfaces. In most cases, crystallites had well-defined tetragonal habits identical to those of larger crystals, which allowed for the easy identification of the length and width for each particle, as illustrated in Figure 2C.

Crystal Structure Determination. X-ray powder diffraction of the micro- and nanoprotein crystals was completed to analyze crystal structure and quality. A 30−50 μL suspension of powder crystalline samples in ultrapure water was packed into 1 mm quartz capillary tubes by centrifugation (1 min, 1000*g*). The packed crystals were approximately 1−2 cm in height, providing an area large enough for X-ray analysis. Crystallographic data was collected on an R-Axis IV^{2+} image plate mounted on a Rigaku X-ray generator (Cu Kα = 1.54 Å). The Crystal Clear software package, 1.3.5SP1g, was used to measure the *d* spacings of the powder diffraction rings. The measurements were taken at room temperature while oscillating the sample 90° with a 1-h exposure time and a sample to detector distance of 450 mm.

The measured *d* spacings from these micro- to nanoprotein crystals were compared to the reflections found for large tetragonal lysozyme crystals grown under conventional conditions. An agate mortar and pestle were used to grind these large tetragonal crystals (not cross-linked) into a protein crystal slurry that could be loaded into capillary tubes. Additionally, the *d* spacings for a powder pattern of tetragonal lysozyme were calculated from known tetragonal unit cell parameters (space group (96), a = 79.10 Å, c = 37.90 Å), which were obtained from coordinates of entry 6LYZat the Brookhaven Protein Data Bank.[22,23] These calculated *d* spacings were compared to measured *d* spacing in order to index each measured ring.

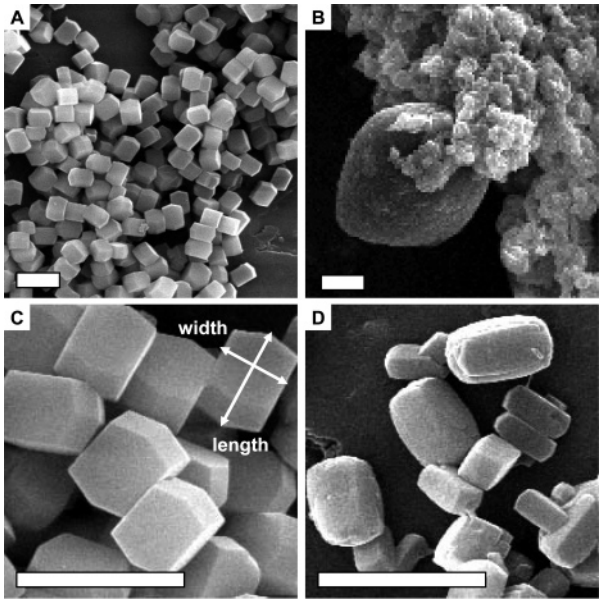

Figure 2. SEM micrographs representative of crystals produced under these similar conditions. The scale bar in these images is 4 μm. The sample in images A and C was centrifuged before cross-linking and contained 6% PEG. Sample B was simply diluted with a cross-linking solution and with no centrifugation. The last image (D) was typical of crystals that were centrifuged before cross-linking but contained no PEG.

Results and Discussion

Method To Produce Submicrometer Protein Crystals. The focus of this work was to discover methodologies for quickly producing high-yield micrometer- to nanosized protein crystals with uniform distributions. Figure 2A and 2C show the typical crystals which form under these low solubility conditions with addition of a PEG additive and with purification by centrifugation. Crystals are uniform with well-defined edges and morphology, as shown in Figure 2C. Additionally, the crystallite size is nearly monodisperse; in this example, the crystals have a size distribution under 10%.

A critical step for most applications of biomolecular crystals is the development of sturdy, strong materials which can be easily handled. In this case, it requires covalently cross-linking proteins within the crystal using glutaraldehyde.[24] When treating the protein crystals it is necessary to minimize any free protein in solution so as to avoid cross-linking of free proteins, which results in amorphous protein aggregates, which can foul the sample. This is accomplished not only by reducing the solubility of the protein itself but also by using centrifugation to isolate the crystals after growth. Figure 2B shows a typical image of material that has not been purified, where the sample was only diluted for the cross-linking procedure to reduce the overall protein concentration. Free protein aggregates are apparent as ill-resolved deposits that obscure the crystalline material

(21) Blundell, T. L.; Johnson, L. N. *Protein Crystallography*; Academic Press Inc.: London, 1994; p 69.
(22) Diamond, R. *J. Mol. Biol.* **1974**, *82* (3), 371−391.
(23) http://www.rcsb.org/pdb/.
(24) Li, Z. Y.; Zhu, W. *Chin. J. Org. Chem.* **1999**, *19* (3), 242−248.

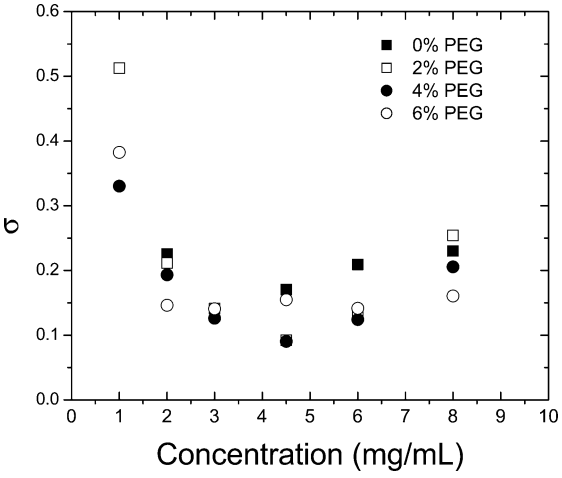

Figure 3. Percent standard deviation (σ) of the crystal width with respect to varying protein and PEG concentrations. The controlled conditions are 3 °C, pH = 3.5, 15% NaCl, and 1 mL batch size.

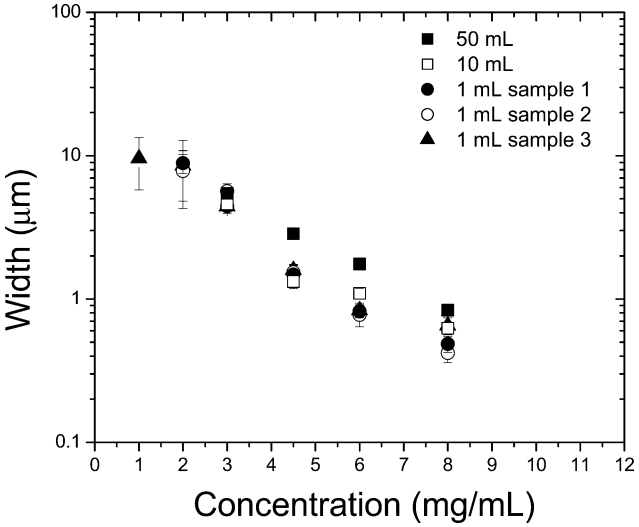

Figure 4. Crystal width plotted as a function of protein concentration. The 1 mL samples 1, 2, and 3 were identical. All crystals were grown at 7 °C, pH = 3.5, 15% NaCl, and 6% PEG.

underneath. In contrast, Figure 2C shows a sample where removal of free protein was complete.

Striking features of many protein nanocrystal images include the presence of sharp edges and observation of nearly monodisperse crystallites (e.g., Figure 2C). These results could only be achieved with the addition of PEG to the crystal growth solution. Figure 2D illustrates that without the addition of PEG protein crystals are polydisperse and have rounded edges with significant etch defects. Size distribution analyses of crystallites produced with varying PEG 6000 concentrations are shown in Figure 3, where it is apparent that higher PEG concentrations allow for better size distributions with a wider focus range of smaller size distributions. With the addition of PEG, there is also an increased viscosity of the solution which could help to both slow crystallite growth and also protect and stabilize crystals from dissolution before cross-linking. Finally, PEG is known to enhance the nucleation of proteins,[25] which in this case would limit nucleation to shorter periods of time, leading to more monodisperse materials.

This method also has very good reproducibility and relatively good scalability, which is apparent in Figure 4. The reproducibility is illustrated by samples 1−3 in Figure 4, which were grown under identical conditions. The average standard variability between batches of identical volume, which included six different protein concentrations run in triplicate, was 10.2%. Surprisingly, we found that crystallite size exhibited a modest dependence on batch volume. Figure 4 shows that with a 50-fold increase in batch volume there was only a slight increase in the crystals size. This small effect is probably due to the fact that in larger batches protein solutions have slower mixing times when introduced into the crystallization buffer, which could lead to the generation of fewer nuclei. The order in which the two solutions, precipitating buffer and protein buffers, are mixed also has an effect on size. When precipitant buffer (750 μL) is added to protein buffer (250 μL), crystals are systematically twice as small when compared to crystals grown with the reversed mixing order. We attribute this effect to the different diffusivities of both the salt and the protein in solution.

Tuning Crystallite Size and Shape. Size control of protein crystals is important because of its relevance to applications ranging from chromatographic separations to catalysis. Figures 5−7 show how crystal size can be tuned by manipulating the protein concentration, pH, salt concentration, and temperature. A more quantitative analysis of particle size or width while varying specific conditions is displayed in Figure 8. Most of these trends can be understood through simple considerations of crystal nucleation and growth.[26]

The effect of increased nucleation is evident for pH (Figure 5), salt concentrations (Figure 6), and temperature (Figure 7); as protein concentration is increased from left to right in these figures, the crystallite size decreases. This occurs because protein concentration controls the rate of homogeneous nucleation and can thereby affect the overall size of the protein crystals.[26,27] The promotion of protein nucleation causes a decrease in crystal size because there is a total reduction in material available per crystal nuclei. Figure 8 captures this apparent trend in graphical form. Particle sizes decrease by an order of magnitude with only a modest change in initial protein concentration. Ultimately, however, the effect of protein concentration was less pronounced at the highest concentration and particle sizes were effectively limited to 250 nm for conditions that favored the smallest crystals. These 250 nm crystals are approximately 45 unit cells in width and 65 unit cells in length.

Other parameters such as pH, precipitant concentration, and temperature also affect crystal growth as well, presumably through enhancing or depressing the solubility of the protein. In 1986 Ataka explored this general relationship of protein solubility to crystal growth.[26] For example, an effect of altering the protein solubility can be seen in Figures 5 and 8A. Progression down the columns in Figure 5 shows protein crystallites grown under increasing pH values

(25) Galkin, O.; Vekilov, P. G. *J. Cryst. Growth* **2001**, *232* (1−4), 63−76.

(26) Ataka, M.; Tanaka, S. *Biopolymers* **1986**, *25* (2), 337−350.
(27) Heidner, E. *J. Cryst. Growth* **1978**, *44* (2), 139−144.

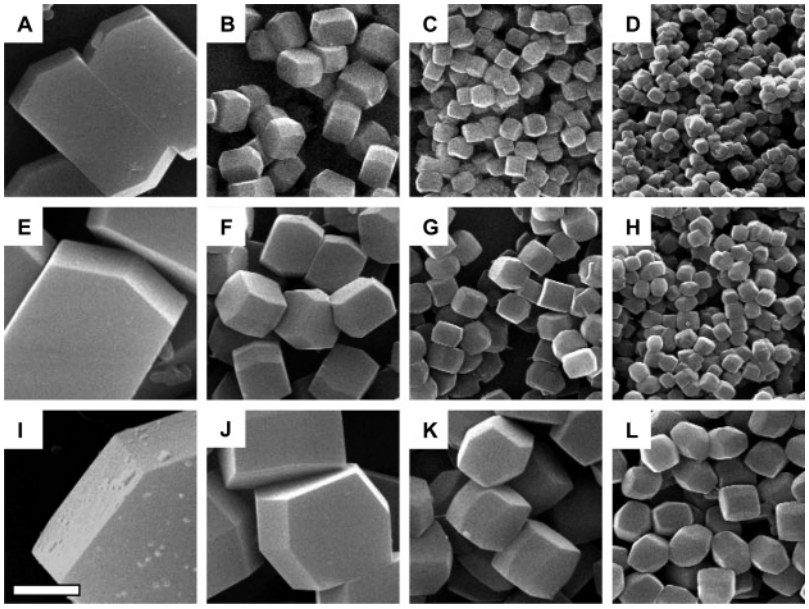

Figure 5. SEM micrographs taken at the same magnification, and scale bar is 2 μm. The above images show the effect of varying pH while maintaining all other conditions (7 °C, 15% NaCl, 6% PEG, and 1 mL batch size). (first row) Samples with pH = 3.0 and protein concentrations of (A) 3.0, (B) 4.5, (C) 6.0, and (D) 8.0 mg/mL. (second row) Samples with pH = 3.5 and protein concentrations of (E) 3.0, (F) 4.5, (G) 6.0, and (H) 8.0 mg/mL. (third row) Samples at pH = 4.0 and protein concentrations of (I) 3.0, (J) 4.5, (K) 6.0, and (L) 8.0 mg/mL.

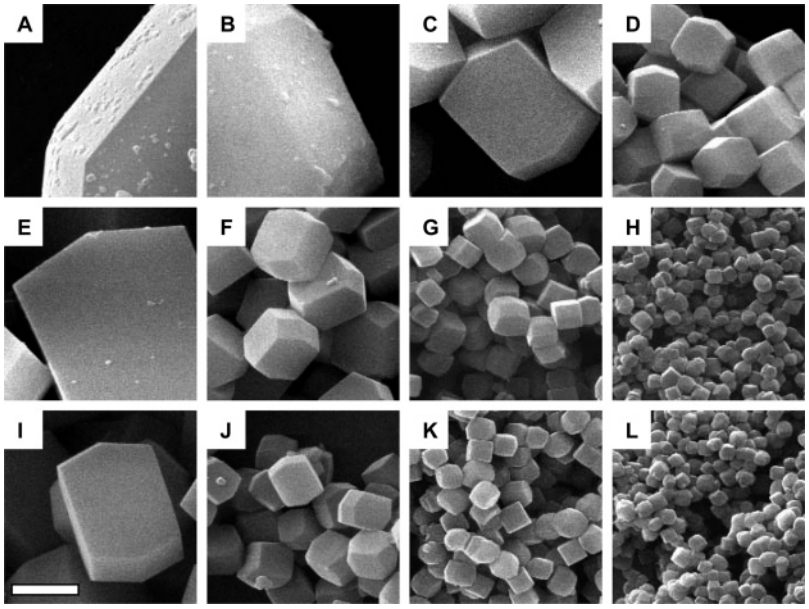

Figure 6. SEM micrographs taken at the same magnification, and scale bar is 2 μm. Effect of varying percent (w/v) NaCl while maintaining all other conditions (pH = 3.5, 7 °C, 6% PEG, and 1 mL batch size). (first row) Samples with 10% NaCl concentration and protein concentrations of (A) 3.0, (B) 4.5, (C) 6.0, and (D) 8.0 mg/mL. (second row) Samples with 15% NaCl and protein concentrations of (E) 3.0, (F) 4.5, (G) 6.0, and (H) 8.0 mg/mL. (third row) Samples with 18% NaCl and protein concentrations of (I) 3.0, (J) 4.5, (K) 6.0, and (L) 8.0 mg/mL.

(pH = 3.0−4.0). Generally, under increasingly acidic conditions, the solubility of lysozyme is greatly diminished.[28] Thus, the smallest crystals result at the lowest pH values, where protein solubility also is lowest.[29]

This strong size dependence due to the change in pH can be understood by considering the effect of protein solubility on crystal size. Conditions that favor lower protein solubility decrease the minimal concentration needed for nucleation to occur and cause a substantial increase in the total number of nuclei formed.[29] Another benefit of using pH to generate low protein solubilities is the reduction in magnitude of the metastable growth region.[28,30] On a protein phase diagram the metastable region is the range of protein concentrations bounded at the upper limit by the concentration needed for protein nucleation and at the lower limit by the solubility of the protein. This can be described as a growth region for protein crystals, and as the pH is lowered to reduce the solubility of the protein, the magnitude of the growth region shrinks.[30] This favors the generation of smaller crystallites by enhancing nucleation as well as limiting growth.

(28) Cacioppo, E.; Pusey, M. L. *J. Cryst. Growth* **1991**, *114* (3), 286−292.
(29) Judge, R. A.; Jacobs, R. S.; Frazier, T.; Snell, E. H.; Pusey, M. L. *Biophys. J.* **1999**, *77* (3), 1585−1593.
(30) Carpineti, M.; Piazza, R. *Phys. Chem. Chem. Phys.* **2004**, *6* (7), 1506−1511.

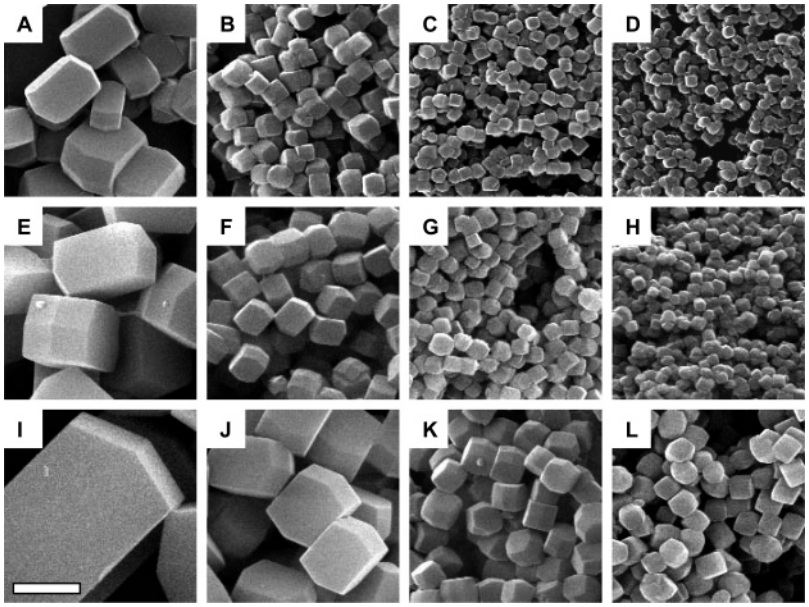

Figure 7. SEM micrographs taken at the same magnification, and scale bar is 2 μm. Effect of varying temperature while maintaining all other conditions (pH = 3.5, 15% NaCl, 6% PEG, and 1 mL batch size). (first row) Samples grown at 1 °C and protein concentrations of (A) 3.0, (B) 4.5, (C) 6.0, and (D) 8.0 mg/mL. (second row) Samples grown at 3 °C and protein concentrations of (E) 3.0, (F) 4.5, (G) 6.0, and (H) 8.0 mg/mL. (third row) Samples grown at 7 °C and protein concentrations of (I) 3.0, (J) 4.5, (K) 6.0, and (L) 8.0 mg/mL.

Similarly, these two effects of increased nucleation and reduction of the growth region can be seen with increased salt concentrations (up to 18 w/w %). In Figures 6 and 8B it is apparent that increasing the salt concentration leads to smaller particles. Little is known about the phase diagram for lysozyme at these high salt concentrations; however, the solubility has been found to decrease by a factor of one-half when increasing salt concentrations from 5% to 7% NaCl at a pH of 4.0.[28,31] Although this trend is not linear, it is expected that the protein solubility will continue to diminish as the salt concentration increases from 10% to 18% NaCl. The increasing ionic strength, again, has the desired effect of reducing the overall magnitude of the metastable region[28,30] and encouraging nucleation.

Changes in temperature also influence protein crystal size, but in this instance the size dependence is likely due only to the temperature effect on the protein solubility. Particle size decreases substantially as does the protein solubility at lower temperature, which can be seen in Figures 7 and 8C. The change in lysozyme solubility drops 8−10% per degree, which is valid over a temperature range of 2−30 °C.[28,31] It is important to mention that a change in temperature does not alter the magnitude of the metastable region.[30] However, the decrease in solubility with lower temperatures would imply that the critical concentration for nucleation also decreases. This would greatly encourage nucleation, causing the same size effect as observed with the other parameters, protein concentration, pH, and salt concentration.

Significant changes in crystal aspect ratios were also observed in all experiments. Figure 9 shows that crystals with smaller aspect ratios were produced when increasing protein concentration. This point has been noted in general studies of lysozyme crystal growth under lower salt conditions.[29,32] A connection between aspect ratio and solubility was more complex. When varying temperature and NaCl concentrations, the aspect ratio decreases as the solubility is decreased. However, pH shows a different trend when aspect ratios increase with decreasing pH, which Judge et al. reported under more conventional crystal growth conditions.[29] This was likely caused by the effect of pH on the surface charge of the protein. Difference in charge could translate into differential growth rates between the {101} and {110} faces of tetragonal lysozyme crystals.

Characterization and Quality of Materials. The habit of these materials suggests not only that they are crystalline but also that they share the same tetragonal symmetry as their bulk counterparts. More concrete verification of crystal quality was found by powder diffraction (Figure 10). Figure 10A shows a powder diffraction image taken from a sample whose average size, as determined by scanning electron microscopy, measures approximately 800 nm. Figure 10B is a pattern obtained from ground protein crystals grown under standard conditions known to produce larger (~200 μm) tetragonal lysozyme crystals. These reflections of the standard and nanoscale crystals are an exact match in dimension and intensity out to *d* spacings of 3.0 Å.

Table 1 summarizes the largest *d* spacings as calculated for a tetragonal lysozyme crystal and compares them quantitatively to measured reflections for nanoscale and standard crystals. The two measured *d* spacings are extremely close and within error for this method of measurement. Additionally, the unit cell dimensions of the nanoscale crystals were calculated (a = 79.05 Å and c = 37.96 Å) and compared to the calculated unit cell dimensions of the standard ground lysozyme crystal (a = 78.84 Å, c = 37.46 Å) and literature values (a = 79.10 Å, c = 37.90 Å).[22] Both sets of calculated unit cell parameters were within 1% of

(31) Forsythe, E. L.; Judge, R. A.; Pusey, M. L. *J. Chem. Eng. Data* **1999**, *44* (3), 637−640.

(32) Durbin, S. D.; Feher, G. *J. Cryst. Growth* **1986**, *76* (3), 583−592.

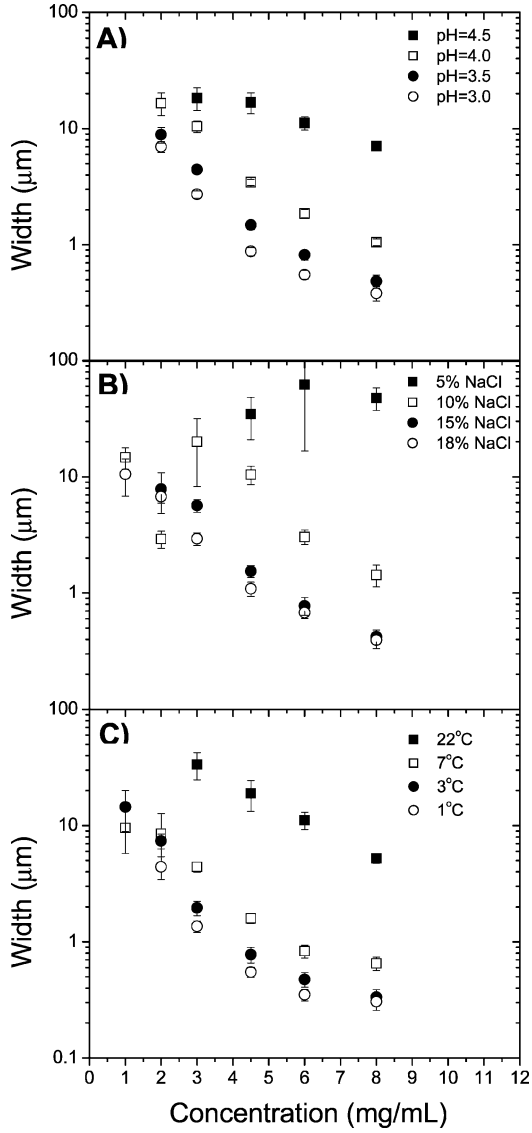

Figure 8. Varying conditions by pH (A) with constant 7 °C, 15% NaCl, 6% PEG, and 1 mL batch size), percent (w/v) NaCl (B) with constant pH = 3.5, 7 °C, 6% PEG, and 1 mL batch size, and temperature (C) with constant pH = 3.5, 15% NaCl, 6% PEG, and 1 mL batch size. The width of the crystals is defined as the distance between the {110} faces.

Table 1

hkl	calcd (Å)	800 nm crystals (Å)	tetragonal lysozyme (Å)
(200)	39.55	39.73	39.51
(210)	35.37	35.14	35.22
(111)	31.38	31.37	31.33
(220)	27.97	27.76	27.87
(211)	25.86	25.63	25.31
(221)	22.50	22.56	22.36
(311)	20.88	20.97	20.81
(400)	19.78	19.91	19.69
(102)	18.43	18.45	18.40

the literature values. Interestingly, the X-ray diffraction resolution of these small crystals was 2−3 Å, and this was comparable to the scattering resolution found for equivalent larger cross-linked HEWL crystals.

The crystal quality was also assessed on the basis of monodispersity and integrity of the crystal shape. At lower initial protein concentrations, higher size distributions were observed. Durbin et al. showed that at these low protein concentrations there were much larger variations between

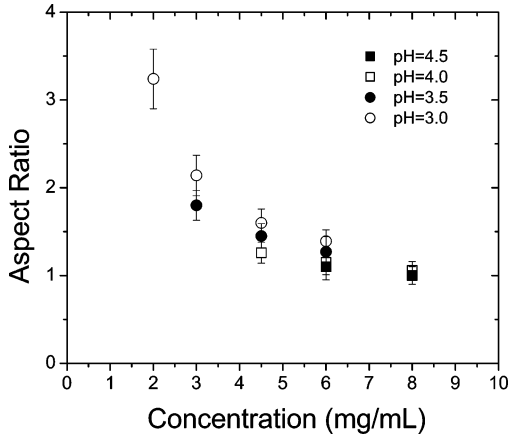

Figure 9. Varying conditions by pH with constant 7 °C, 15% NaCl, 6% PEG, and 1 mL batch size. The aspect ratio is length divided by width. In this case the length is the distance between the apexes of the {101} faces and the width is the distance between the {110} faces.

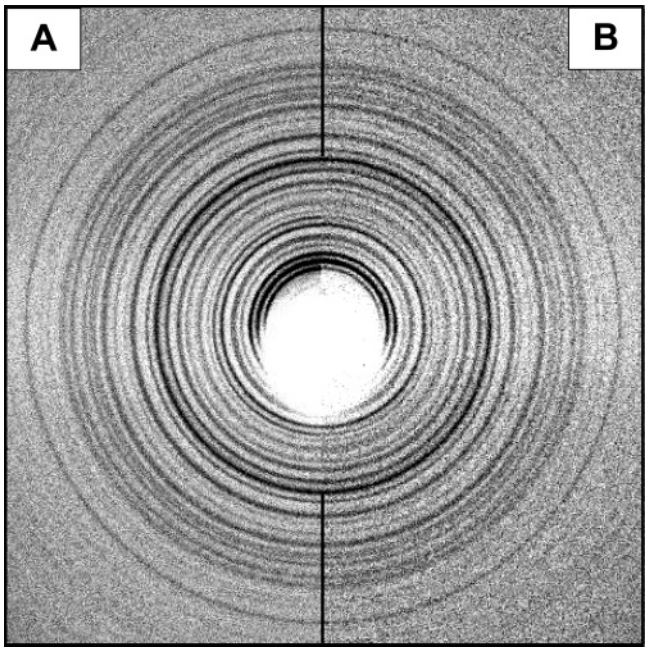

Figure 10. Powder diffraction of 800 nm protein crystals (A) matches the powder diffraction form standard tetragonal lysozyme crystals (B). These two patterns have identical reflection intensities and *d* spacings.

growth rates of crystals within the same batch.[32] These differences in growth rates can lead to crystals with dramatically larger size distributions. It should also be noted that the lowest solubility conditions coupled with higher protein concentrations appeared to form crystals with more rounded edges and twin defects. This could be explained by the rapid growth caused by these extreme levels of protein saturation, which would inherently form more defective or less uniform crystals.

As in the development of any synthesis strategy, this method was designed to generate materials with efficiency and high yields. Quenching strategies, for example, may produce small-scale crystallites, but this approach leaves much of the initial protein in soluble form. Our approach was to control crystal size through growth conditions which accelerate nucleation under very low protein solubility. This correlates to faster growth rates. As a result, for most conditions, nearly all of the available protein is used in the

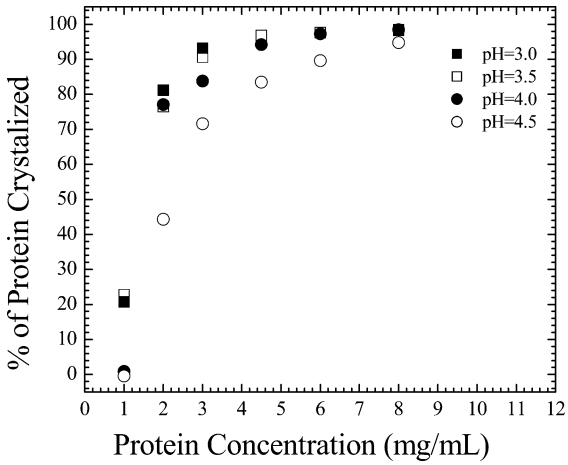

Figure 11. UV absorption measurements taken on the supernatant of the centrifuged batches to determine the percent yields of protein crystals. The conditions were 7 °C, 15% NaCl, 6% PEG, and 1 mL batch size with varying pH.

production of crystallites. Figure 11 presents yield versus initial protein concentration. For the highest protein conditions, nearly 100% yields are observed for crystals grown over a period of 24 h. The lower protein concentrations however have lower yields. This observation is due to not only the smaller initial protein concentration to solubility ratio but also the slower growth conditions that did not allow these batches to reach equilibrium.

III. Conclusions

It was possible to make nanoscale to submicrometer HEWL crystals at very low protein solubility. This method has good reproducibility with high yields resulting in little loss of protein. The size and shape is tunable through rational manipulation of growth conditions that control protein solubility and the initial protein concentration. Higher protein concentrations and conditions that favor lower solubility give smaller protein crystals. The quality of the nanocrystals grown at these elevated growth rates was still relatively good, with an X-ray diffraction resolution of 2−3 Å. The method is relatively scaleable and could produce more reliable results for the larger batch volumes if a more efficient transfer of solutions is implemented. Smaller protein crystals with dimensions well under 250 nm (∼50 unit cells) were not easily formed by this method, and their production is the subject of ongoing efforts.

Acknowledgment. This research was supported by NSF (CHE-0103174) and ONR (N00014-04-1-0003). We thank Professors Yizhi Jane Tao and Yousif Shamoo along with his entire lab for their insights and use of their X-ray diffractometer.

CM047924W